

Received April 29, 2020, accepted May 27, 2020, date of publication June 8, 2020, date of current version June 26, 2020.

Digital Object Identifier 10.1109/ACCESS.2020.3000599

# Cognitive Intelligence for Monitoring Fractured Post-Surgery Ankle Activity Using Channel Information

ARNAB BARUA<sup>1</sup>, ZHI-YA ZHANG<sup>1</sup>, FADI AL-TURJMAN<sup>2</sup>, (Member, IEEE), AND XIAODONG YANG<sup>1</sup>, (Senior Member, IEEE)

<sup>1</sup>School of Electronics Engineering, Xidian University, Xi'an 710071, China

<sup>2</sup>Research Center for AI and IoT, Department of Artificial Intelligence Engineering, Near East University, 99138 Nicosia, Turkey

Corresponding authors: Zhi-Ya Zhang (zyzhang@xidian.edu.cn) and Xiaodong Yang (xdyang@xidian.edu.cn)

**ABSTRACT** In the past decades, cognitive computing and communication densely used in lots of networking areas. Current improvement in deep learning (DL) and big data analysis create great potential to analyze cognitive intelligence (CI) for many applications such as human activity monitoring and recognition through wireless communication. Cognitive intelligence and wireless communication are using to establish smart healthcare systems. Healthcare monitoring systems turn into interesting research subjects where monitoring post-operative surgical patients are the current focal point to the researcher. In this paper, we argue that deep learning along with the wireless communication technique introduces cognitive intelligence for the healthcare monitoring system. We present a deep learning based convolutional neural network (CNN) model to classify image data and a convenient and multi-functional software-defined radio (SDR) platform to detect movement of the ankle of patients who underwent ankle fracture surgery. Capturing wireless channel state information (WCSI) in the presence of the human body and classifying using CNN to observe distinct movements is the key idea of this study. A universal software radio peripheral (USRP) platform used to capture WCSI data and used for classification. AlexNet and ZFNet both are the famous architecture of CNN and used in a parallel way to classify captured WCSI-based images that converted from numeric data. The classification established on the ankles movements after surgery and classification results show that CNN provides satisfying results where test accuracy is 98.98%.

**INDEX TERMS** Cognitive intelligence, DL, CNN, USRP, WCSI, AlexNet, ZFNet, post-surgery.

## I. INTRODUCTION

In the last few years, huge development in AI, software, and hardware technologies make cognitive intelligence (CI) famous in academics and industry. Terms of cognitive computing or intelligence stand for hardware and software systems that follow the functions of the human brain and enhance decision-making [1]. A cognitive system, i.e., Watson, developed by IBM Corporation, which learns from documents without any supervision. Adaptive, interactive, iterative, stateful, and contextual are considered as features of cognitive intelligence [2]. The concept of cognitive intelligence used to build applications like smart city [3], smart healthcare [4], smart transportation [5]. It also earned serious

attention in modern networking and communication. Nowadays, researchers focused on the use of cognitive systems to utilize wireless channel information properly. In this research, we use the concept of cognitive intelligence for monitoring. Cognitive intelligence used in health monitoring because of its several aspects and more found in [6]–[8].

Currently, researchers have exposed their interest in the health area, as there is a huge chance to support human lives by monitoring or detecting diseases. Monitoring post-surgery patients is a positive research area because regular monitoring of the patient's health status is compulsory to prevent any loss [9], [10]. Ankle fracture is one of the most common in bone and joint injuries. Sometimes surgery is necessary to fix ankle fracture. After ankle surgery, 30% to 70% of patients will experience chronic ankle instability [10]. To avoid chronic ankle instability after ankle surgery, patients go to

The associate editor coordinating the review of this manuscript and approving it for publication was Min Xia<sup>1</sup>.

the physical therapists for best ankle exercises to improve the condition. By doing the exercises and monitoring the ankle movements, it is possible to ankle rehabilitation [11], [12]. It is not always possible to go to the therapists for the checkup of the improvement of ankle movements after performing exercises. In this research work, we try to solve this issue by using the monitoring technique. Nowadays, various sorts of excellent hardware and approach used for monitoring purposes in real-time.

Camera, infrared sensor, light sensor, accelerometer, pressure sensor, and many more hardware systems used for monitoring movements though all are not always convenient to use in all positions [13]. Improvement of wireless signal technology helps wireless sensing to be famous as a device-free technology and solve problems that are related to hardware [14], [15]. Wireless signals useful for monitoring and can detect the activities of humans at the hospital, home, and bedrooms. Human movements create perturbation, which affects the WCSI of the wireless signals. It has advantages over the camera, sensors to detect human movements. In this study, we are using WCSI for monitoring patient's post-surgery ankle movement. Lots of hardware-based platforms used to capture WCSI. In this research, we used an SDR based platform like prior research works [16], [17]. To upgrade the monitoring efficiency of hardware devices, different kinds of classification algorithms developed.

In this paper, we note that the improvement of DL creates possibilities of cognitive ability of wireless technology for proper identification. DL is known as a subset of machine learning (ML). In deep learning, a deep architecture buildup with multiple layers, and every layer executes a non-linear transformation on the outputs of the previous layer [18], [19]. Supervised and unsupervised, both types of data can classify by using deep learning. Convolutional neural network (CNN) is one of the famous models of deep learning, which is also known as a multilayer feedforward artificial neural network, and it widely uses in image processing, computer vision, video detection, and natural language processing [20]–[22]. The convolution network consists of shared weights and to achieve high translation invariance, only weighty features of the data use [23]. Prior research works like [24]–[27] used simple CNN model instead of complex model to classify wireless data. In this paper, we are using AlexNet and ZFNet, two renowned architecture of CNN in a parallel manner to classify data. The use of two architecture makes the CNN model complex to build. We convert WCSI data into images and fed into the CNN model to detect ankle movements of post-surgery ankle fractured patients.

DL has seen its popularity during the last few years because its applications spread every industry and research area [28]–[30]. The main reason is the development of the correct and multipurpose system, which enables algorithm design to work with information theory and signal processing along with better performance. The availability of robust DL libraries and special hardware like graphic processing unit (GPU) and field-programmable gate array (FPGA) is

another reason. For real-time signal processing applications, those reasons are necessary for the training and assumption of DL models. Currently, different research teams started exploration beneath DL based applications in signal processing and communications such as compressed sensing [31], detection for multiple-input multiple-output (MIMO) systems [32], detection algorithms for molecular communications [33].

Our research work has feasibility in clinical and practical situations. In the clinical situation, doctors can monitor the ankles movement and can understand the ankle's situations. In the practical situation, it helps a patient to acknowledge the current situation of ankles after doing exercises without visiting any doctors or physicians. While doing exercise, our system can notify patients which exercise they are performing and how well they are performing exercises, which make our system user friendly.

Contribution of this research work given below:

- 1) This research work used cognitive intelligence for monitoring and detecting multiple activities.
- 2) We apply two separate CNN architecture in this research in a parallel manner to increase the classification accuracy.
- 3) In this research work, we classify images instead of numerical data, which are more reliable.
- 4) This work assists post-surgery ankle fractured patients to know the status of the ankles movement with the help of monitoring.
- 5) This research work helps to contribute to many health care monitoring systems via the USRP platform.

The outline of this paper as follows, Section 2 describes the motivation of the work, Section 3 discusses related works, Section 4 describes the system model, Section 5 describes the methodology of the work, Section 6, contains the experimental result and discussion and Section 7 concludes the paper. In the following Table 1, we summarize all the used acronyms and abbreviations in this work to assist the reader.

## II. MOTIVATION

In prior works, the use of cameras, radars, and wearable devices are familiar with monitoring human activity, though lots of difficulties come out to use them [34], [35]. Monitoring ankles movements of post-surgery ankle fractured patients are possible with the help of wireless signals. WCSI and received signal strength (RSS) are the components of wireless signals and WCSI based on orthogonal frequency division multiplexing (OFDM), which broadly used to gain elegant multipath information [14], [36]. The human body build-up with water and wireless signals reflect the human body easily; that why the human body motion easily detectable by WCSI [37]. These reasons motivate us to use the WCSI technique than cameras, radar, sensors, and wearable devices technique for monitoring purposes. One major concern in classification is to increase accuracy; that why data pre-processing is necessary before classification. Raw numeral data from WCSI always contain noise, but instead of using

**TABLE 1. List of used acronyms and abbreviations with the definition.**

Acronyms and Abbreviations	Definition
DL	Deep Learning
CI	Cognitive Intelligence
CNN	Convolutional Neural Network
SDR	Software Defined Radio
WCSI	Wireless Channel State Information
USRP	Universal Software Radio Peripheral
ML	Machine Learning
RSS	Received Signal Strength
FMCW	Frequency Modulated Continuous Wave
CW	Continuous Wave
LOS	Line of Sight
NLOS	Non Line of Sight
PCA	Principal Component Analysis
SVM	Support Vector Machine
k-NN	k-Nearest Neighbor
DT	Decision Tree
ORIF	Open Reduction and Internal Fixation
MIMO	Multiple Input Multiple Output
FDD	Frequency Division Duplex
TDD	Time Division Duplex
ANN	Artificial Neural Network
ReLU	Rectified Linear Unit
DUC	Digital Up-Conversion
DAC	Digital to Analog Conversion
LPF	Low Pass Filtering
TA	Transmit Amplification
LNA	Low Noise Amplification
ADC	Analog to Digital Converter
DAC	Digital to Analog Converter
LPA	Log-periodic Antenna
QPSK	Quadrature Phase-Shift Keying
PR	Precision
RE	Recall
MCC	Mathews Correlation Coefficient
TP	True Positive
TN	True Negative
FP	False Positive
FN	False Negative
TPR	True Positive Rate
TNR	True Negative Rate
ROC	Receiver Operating Characteristics
GPU	Graphic Processing Unit
FPGA	Field Programmable Gate Array

numeral data, plotted WCSI numeral data converting into image data is a good solution. In the WCSI based image data, no need to use data preprocessing methods which motivate to use image data instead of numeral data. Machine learning algorithms used to classify data to recognize human activity but accuracy not always satisfactory [13], [38]. CNN models largely used in image classification-based research and earned vast fame in increasing accuracy which

is another motivation to use CNN instead of the ML-based algorithm.

Researchers are focus on developing systems by using SDR based special hardware like USRP and image processing methods. Among lots of platforms, SDR based platforms famous for using capturing accurate WCSI data [16], [17], [24]–[27], which motivated us to use. However, preparing an SDR platform is always challenging because hardware error and data error can show up at any moment. Our main concern on image classification that why we focus on building a proper CNN model to achieving better accuracy results. In a few prior research works like [16], [17], [24]–[27], SDR based hardware platform used to classify wireless signals using the CNN model. However, their designed CNN model is simple and not let them achieve high accuracy. The complex CNN model always helps to get high accuracy that motivates us to design our CNN model in a complex way, but designing a complex model is always a key challenge. A complex model always time-consuming and face high training and validation error. Our article has significance in communication and computational efficiency. One significance in communication and computational efficiency stays in the SDR platform based USRP hardware because it can communicate and transfer data more efficiently than other wireless techniques as well as compute data accurate way for further processing. Another significance in computational efficiency lies in the CNN model. The computation time of our CNN model for training is lower and can provide an acceptable result. Our article has significance than other approaches like no need to wear like wearable sensors, no need to fix special places like floor sensors, no need to concern about lighting or blocking staff like camera techniques, can easily set up than radar technology.

### III. RELATED WORKS

Previously, researchers performed different sorts of experiments for monitoring human activities using different types of schemes and techniques. In this section, we concisely discuss related works on camera-based, sensor-based, radar-based, hardware-based, Wi-Fi-based, and classification-based.

#### A. CAMERA BASED

Because of the concept of computer vision, image processing, object detection using camera make monitoring human activity famous to the researcher [39]. In [40], a camera-based technique used with the USF Human ID database and earned 91% accuracy. In [41], they recorded human movement using a camera to analyze human silhouette for recognition and monitoring and earned 93% accuracy. Using the camera is a good technique but still has some complications such as no noise in the experimental area, the proper facility of good lighting, and concerning camera-blocking staff. In our study, we use wireless signals for monitoring, which is better than camera-based techniques because there is no need to concern about lighting, noise, and blocking staff.

## B. SENSOR BASED

Sensors are famous for using monitoring purposes because of their availability. In [42], a wearable sensor used to monitoring activity and achieved 80% to 90% accuracy. In [43], the used floor sensor to recognize a single human in an empty area and achieved 90% to 97% accuracy. Sensors need to set up in a specific way to achieve good accuracy results, and peoples always not feel comfortable wearing sensors, so those considered as limitations. In our WCSI based work, no need to concern about wearable staff, and setup is easier than sensors.

## C. RADAR BASED

Radar technology is famous among researchers for monitoring human activity because human motions possible to identify by using the Doppler shift of the reflected signal with the help of frequency modulated continuous wave (FMCW) radars [13]. In [44], they used continuous wave (CW) radar, which depends on the Doppler signature for monitoring human activity and gained 95% accuracy. In [45], they used FMCW radar to monitoring humans behind the wall, and they gained 88% accuracy. Our scheme based on wireless signals, which are easier to use than radar signals, and we used 5.32 GHz, which is lower than 10.525 GHz of CW radar [46]. The setup of the wireless signal devices is easy, and the operation cost is lower than the radar signals.

## D. HARDWARE BASED

Improvement of hardware technology increases the researcher's interest in using them in monitoring human activity. In [47], they earned 88% accuracy to monitor human activity by designing an analog circuit. In [48], they detected human involuntary movements by using the PHAN-ToM Omni device and earned 90% accuracy. In comparison with [47], [48], we used the USRP device to collect WCSI data, which is faster, easy to use, and provides better accuracy.

## E. WI-FI BASED

In the field of device-free sensing, researchers use Wi-Fi signals for sensing human activity [49]. Wi-Fi sensing possible to apply for both LOS and NLOS environments. In [50], they used the Intel 5300 wireless network interface card and applied the Orthogonal Frequency Division Multiplexing (OFDM) modulation technique to monitoring human fall and achieved 87% accuracy. In [51], they used the same network interface card like [50] and captured WCSI histogram to monitoring human walking and earned 92% accuracy. Compared to other schemes, we used a USRP device based on the SDR platform and capture WCSI to monitor the ankles of post-surgery ankle fractured patients, which is more sensitive and provides good results.

## F. CLASSIFICATION BASED

Researchers justify the accuracy of their used schemes by classifying collected data using several algorithms.

In [12]–[14], they classify WCSI data using principal component analysis (PCA), support vector machine (SVM), k-nearest neighbor, and decision tree (DT) algorithms and gained accuracy result in between 93% to 97%. In [34], they designed a CNN model to classify WCSI data to monitoring human respiration and earned 94% accuracy. In this work, we used two renowned architecture of CNN and ran them in a parallel way to classify WCSI based image data.

## IV. SYSTEM MODEL

In this section of this paper, we discussed our system model. We present a typical design of our proposed system model in Figure 1. We divided our system model into five parts. The relevance between the five parts and cognitive computing presented here.

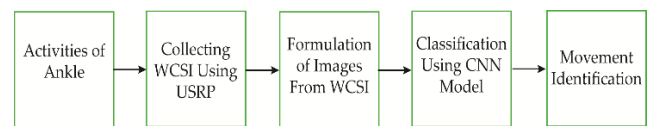


FIGURE 1. Typical design of the proposed system model.

### A. ACTIVITIES OF ANKLE

In the human body, the ankle joint is one of the main weight-bearing structures. Ankle's function and structure are different, and people's ankle often injured because of careless jumping, landing, or vehicle accidents. It estimated that two million people get admission to hospital by ankle fractures every year [52]. Generally, in sports, the most common injury is ankle sprain and the risk of an ankle sprain is increase for the athlete if he/she already experienced it [53]. Athletes can face serious chronic pain and disability because of an ankle sprain. Ankle joint makes up with three bones, and they are the tibia (shinbone), the fibula (the smaller bone in the human leg), and the talus (a bone in human foot). Injury can damage the lower tibia, lower fibula, or talus, and because of injury, only one of three bones might break or might have a fracture in two or three bones. In the types of fractures, one types in a human bone break into pieces and it's possible to line up correctly; another type is because of injury human bone fragments move out of its alignment. Ankle fractures commonly categorized as lateral malleolus fracture, bimalleolar ankle fracture, trimalleolar ankle fracture, and pilon fracture [54]. An ankle fractured or sprain patient can feel several symptoms and they are severe pain, swelling, bruising, tender to touch and deformity [55]. Patients can recover injury by using the nonsurgical treatment and surgical treatment. Most ankles fractured patients need to go through open reduction and internal fixation (ORIF) surgery to stabilize and heal fracture [56]. After surgery patients need physical therapy to regain strength and flexibility in the muscles. There are chances of full recovery by doing exercises as prescribed regularly. Physical therapists help patients to choose the best ankle exercise to improve the condition. It is not always possible to meet the physical therapists to show the improvement

of the ankle by doing regular exercises. To solve this problem of post-surgery ankle fractured patients, we proposed our work, which will help them to monitor their ankle movements without the presence of the physical therapists. Monitoring the patient’s ankle activity can be possible based on the repetition of the movement of the ankle and using wireless sensing techniques. In [12], they suggest seventeen exercises for ankle and in this paper, we used ten common exercises of the ankle. After surgery, rehabilitating the ankle should be done slowly and carefully. Before starting any exercise, consultation with a doctor or physical therapist is necessary. In Table 2, we present a list of exercises with their actual names, short names and actions with images.

**B. COLLECTING WCSI USING USRP**

With the help of AI, cognitive intelligence is valuable for wireless sensing technology to improve various kinds of technical challenges. At the same time, wireless technologies and network systems need to upgrade with new features, including 5G network services, which assisted by cognitive intelligence, wireless signal processing using deep learning, adaptive wireless resource management using cognitive power, and so on.



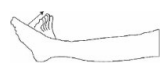





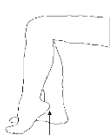

Wireless sensing technology used for monitoring purposes in the healthcare sector because of its reliability [18]. In this research, we used wireless sensing technology at 5.32 GHz and captured WCSI data. Human movements produce a distinct kind of signature in the wireless channel, it allows subcarriers to explain the channel measurement in WCSI scheme, and the received signal is known as,

$$y = Hx + n \tag{1}$$

In Equation 1,  $y$ ,  $H$ ,  $x$ , and  $n$  stand for the received signal, channel information, transmitted signal, and the noise, respectively. Activities performed in the line-of-sight (LOS) to interrupt the wireless signals and the collected data contain subcarrier frequency to symbolize WCSI [51].

In this research, we captured WCSI data using the SDR platform based USRP device. SDR platform puts software closer to the antenna and provides design flexibility and up-gradation possibility. In the research work, several kinds of SDR platforms are using, and USRP is one of them which is developed by Ettus Research (a National Instruments Company) [57]. USRP is famous for using in various sorts of research work [58]–[61] and education [62]–[67]. We used the USRP B210 bus series Ettus Research with two independent transceivers, which allow implementing a multiple-input and multiple-output (MIMO) system. It covers frequency from 70 MHz to 6 GHz with the bandwidth of 200 kHz to 56 MHz, and they can easily run in Frequency Division Duplex (FDD) or Time Division Duplex (TDD) modes. In the transmit path, RFICs AD9361 used, which increases the output power over the wireless channel for sending the signal. The transmit power of this USRP device is changeable, and above 20 dBm is the maximum transmit power, and –15dBm is the receive input power. The maximum gain for

**TABLE 2. List of selected exercises with name, action, and pictures.**

Exercise Name	Short Name	Action	Picture
Non-Weight Bearing Dorsiflexion	NWBD	Need to move the ankle and point the foot towards the nose.	
Non-Weight Bearing Flexion	NWBF	Need to move the ankle and point the foot forward	
Non-Weight Bearing Inversion	NWBI	Need to move ankle with keeping toes pointed up and the foot facing to another leg.	
Non-Weight Bearing Eversion	NWBE	Need to move ankle with keeping toes pointed up and turn the foot outward.	
Resisted Strengthening Dorsiflexion	RSD	Need to move the ankle and point the foot towards the nose using a Thera band.	
Resisted Strengthening Planter Flexion	RSPF	Need to move the ankle and point the foot forward using a Thera band.	
Resisted Strengthening Inversion	RSI	Need to move ankle with keeping toes pointed up and the foot facing to another leg using a Thera band.	
Resisted Strengthening Eversion	RSE	Need to move ankle with keeping toes pointed up and turn the foot outward using a Thera band.	
Partial Weight-Bearing Seated Calf Raises	PWBSCR	Need to lift the injured heel as far as possible while keeping the toes on the ground.	
Full Weight-Bearing Single Leg Stance	FWBSLS	Need to stand on the injured foot and lift the uninjured foot off the ground.	

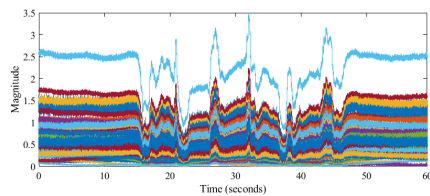
transmitting frontends is 89.8 dB and the maximum gain for receiving frontends is 76dB. In Figure 2, we present a typical

scenario of detecting human movements using wireless signals and the USRP device.

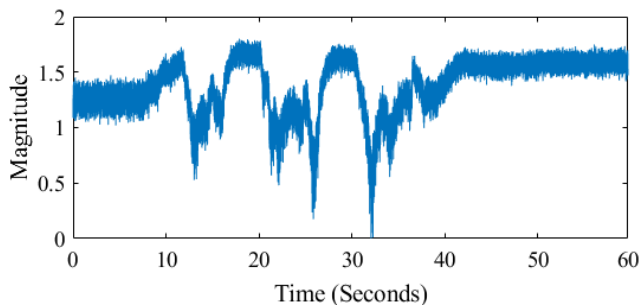


**FIGURE 2.** A typical scenario of detecting movements using USRP and wireless signals.

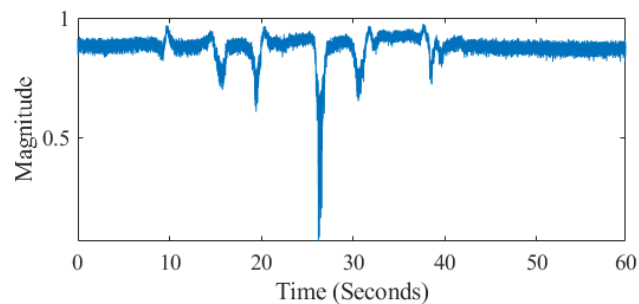
Like Figure 2, human subjects performed ankle activity within the line-of-sight path by following activities of ankle exercise in Table 2. We captured WCSI values from 64 subcarriers. In Figure 3, we presented WCSI values of 64 subcarriers of Non-Weight Bearing Dorsiflexion activity of ankle.



**FIGURE 3.** WCSI waveform of 64 subcarriers.

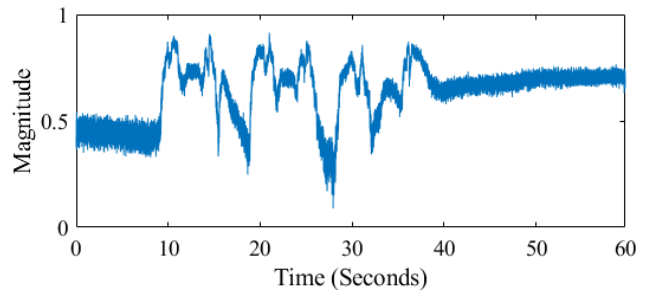


**FIGURE 4.** Captured WCSI waveform of resisted strengthening dorsiflexion in 60 seconds.

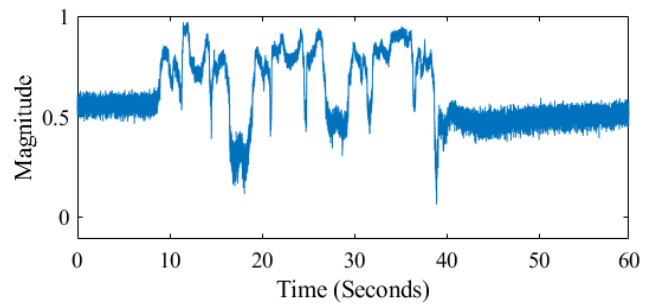


**FIGURE 5.** Captured WCSI waveform of non-weight bearing flexion in 60 seconds.

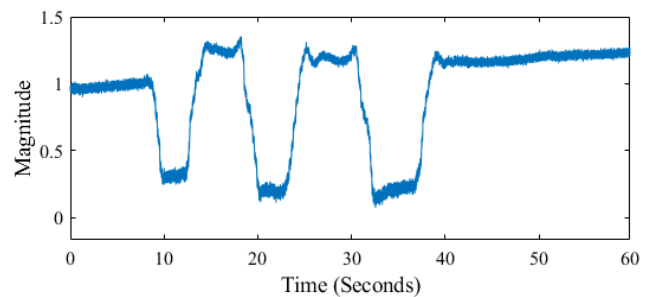
All the activity of the ankle performed in 60 seconds, and we collected 64 subcarriers for all. In Figure 4 to 13, we presented WCSI values of one subcarrier of all activities of ankle exercise followed by Table 2, and all the presented figures help to understand the differences between each activity.



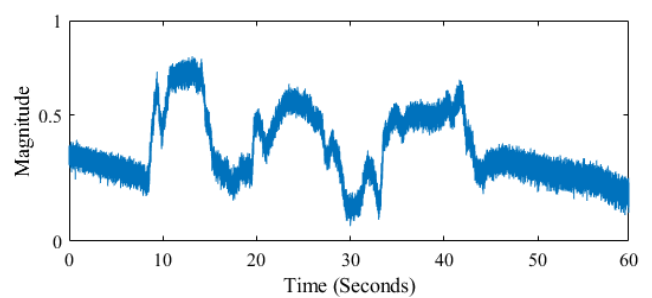
**FIGURE 6.** Captured WCSI waveform of non-weight bearing inversion in 60 seconds.



**FIGURE 7.** Captured WCSI waveform of non-weight bearing eversion in 60 seconds.



**FIGURE 8.** Captured WCSI waveform of resisted strengthening dorsiflexion in 60 seconds.



**FIGURE 9.** Captured WCSI waveform of resisted strengthening planter flexion in 60 seconds.

### C. FORMULATION OF IMAGES FROM WCSI

We generated images by using WCSI numeral data and classify them using the CNN model. After finished the experiment, we used Matlab software to plot every single subcarrier

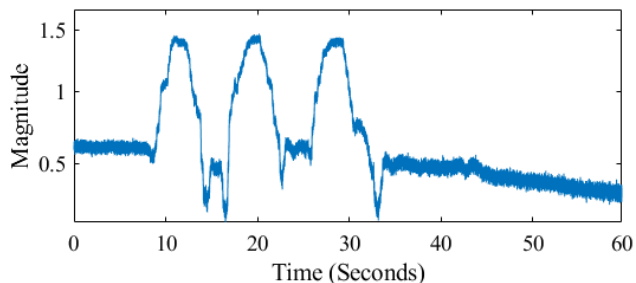


FIGURE 10. Captured WCSI waveform of resisted strengthening inversion in 60 seconds.

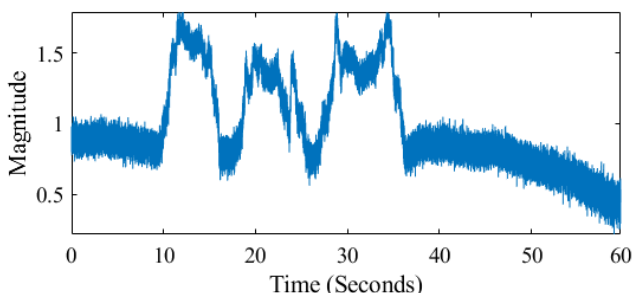


FIGURE 11. Captured WCSI waveform of resisted strengthening eversion in 60 seconds.

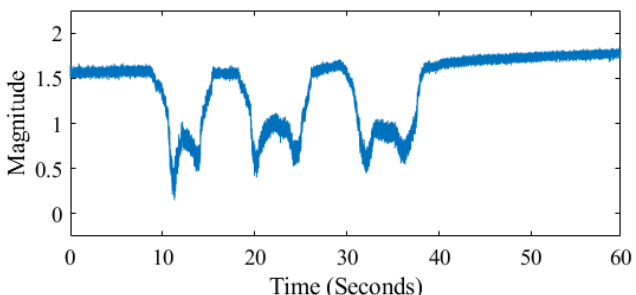


FIGURE 12. Captured WCSI waveform of partial weight-bearing seated calf raises in 60 seconds.

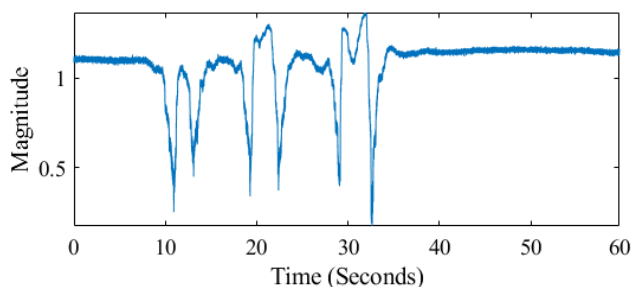


FIGURE 13. WCSI waveform of full weight-bearing single leg stance in 60 seconds.

of all the ankle activities and save them as images in jpg format. In the image, we did not put any word, number except waveform.

In Figure 14, we presented a sample of an image which kind used for classification. After formulated all the images, we collected a total of 32,000 images and split all the images

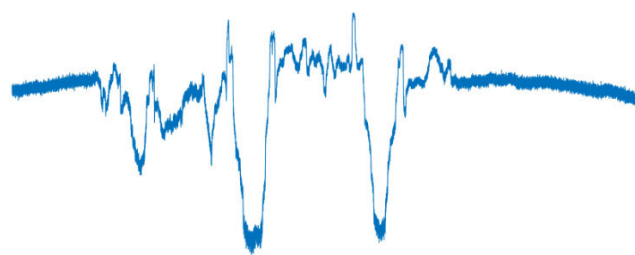


FIGURE 14. Image of activity for classification.

into the train, validation, and test section depend on the percentage where the percentage is 60% train, 20% validation, and 20% test. The process of collecting images describe in the data accumulation section.

#### D. CLASSIFICATION USING CNN MODEL

Using the thinking mode of the human, we can make a solution for real-world problems. Computer applications are getting sophisticated day by day because of the concept of cognitive computing, and the researchers start using those applications to solve complicated problems. Deep learning is an example of proper cognitive computing because in deep learning, the process works like the human brain. Lots of deep learning based available nowadays, and researchers use them to solve several tasks.

In deep learning, the convolutional neural network (CNN) used to learn a convenient portrayal from images that considered as its ability, and nowadays, it is using in monitoring purposes in lots of research papers [22], [68]–[70]. Besides monitoring, deep learning also famous for using in the biomedical sector. In [71], they used CNN with position-specific scoring matrices (PSSM) to recognize electron transport proteins and achieved an accuracy of 92.3%. Their proposed technique can help biologists to understand the function of the electron transport proteins. In [72], they used two-dimensional CNN and PSSM to recognize clathrin proteins from high throughput sequences. The architecture of CNN establishes on computational factors and fundamental mathematical functions. CNN based on two central computational networks, and they are feature learning network and classification network [73], [74]. The feature learning network consists of the convolution layer, pooling layer, and flattening layer and the classification network consists of a bunch of hidden layers and output layers. The classification network sometimes acts as an artificial neural network (ANN). To know more about CNN and its layers, readers can follow [75]–[79] works of literature. In this research, we used two famous architecture of CNN to classify images and they are AlexNet and ZFNet. We run both architectures in a parallel manner to classify all the images. More about AlexNet and ZFNet architecture clarified in the following subsections, which will help to understand our method.

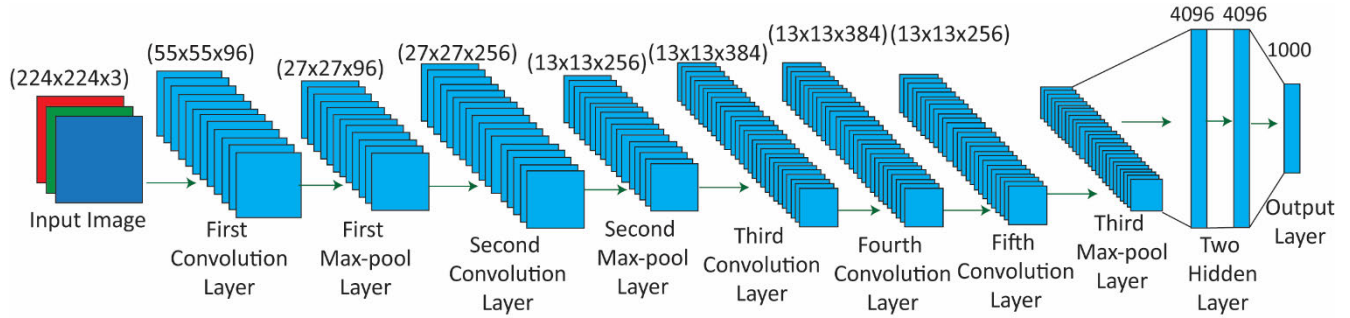


FIGURE 15. The architecture of AlexNet.

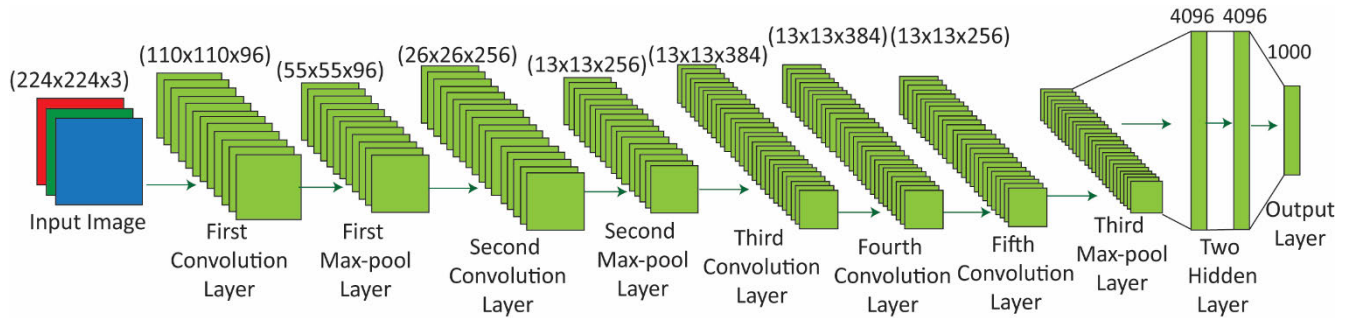


FIGURE 16. Architecture of ZFNet.

1) AlexNet

AlexNet is a renowned architecture of CNN for image classification. This architecture entered in ImageNet LSVRC-2010 and ILSVRC-2012 contest and won the ILSVRC-2012 contest by classifying 1.2 million high-resolution images [77], [78]. To avoid overfitting problems in the fully connected layer, they used the dropout regularization method.

AlexNet consists of eight layers where the first five are convolution and three fully connected layers. Three max-pooling layers used after the first, second, and fifth convolution layers. Originally, the developers of AlexNet split the architecture into two parts in the time of classification, but in our research, we run the whole architecture without splitting. In Figure 15, we presented the architecture of AlexNet.

2) ZFNet

ZFNet comes after AlexNet and also popular in research because of the layers visualization technique [77]. This architecture won the ILSVRC-2013 contest and its better version of AlexNet. The architecture of ZFNet is the same as AlexNet, with some differences in Figure 16, we presented the architecture of ZFNet.

Like AlexNet, it consists of eight layers. The first five are the convolution layer, along with three max-pooling layers and three fully connected layers. The differences between AlexNet and ZFNet are, in the first convolution layer of AlexNet, kernel size is 11, and stride value is 4; in contrast, kernel size is 7, and stride value is 2 in the first convolution layer of ZFNet. From the second to the fifth convolution of

the AlexNet, the stride value is 1; however, the stride value of the second convolution layer is 2 in ZFNet, and the rest is the same as AlexNet. Deconvnet Techniques for visualization introduced by ZFNet, which help to visualize layers status. In this research, we used ZFNet architecture without deconvnet. As the classification network of both architectures is the same, that’s why in this research, we run the feature learning network in a parallel manner then merge both results.

After merge, we fed the result of the feature learning network into the classification network. In Figure 17, we presented the architecture of our convolution neural network.

In our architecture, the number of neurons for the output layer is 10 because we have ten ankle activities, and 10 is our class number. Based on the class number, the number of neurons of the output layer is decide. In the output layer, we used the softmax activation function, and in the hidden layer, we use the rectified linear unit activation function (ReLU). At the output of the convolution layer, we also use the ReLU function. Summary of our CNN model presented in Table 3 and summary will help to understand the parameters of the architecture along with how every layer work.

From Table 3, we can observe that both architectures run in a parallel manner and concatenate the value of both layers after the last max-pooling layer then fed into the hidden layer. Name of each layer given by the model automatically. Five convolution layer of AlexNet named with “Convolution1 to 5” and five convolution layer of ZFNet named with “Convolution6 to 10”. Three max-pooling layers of AlexNet named with “Max-pooling1 to 3” and three max-pooling



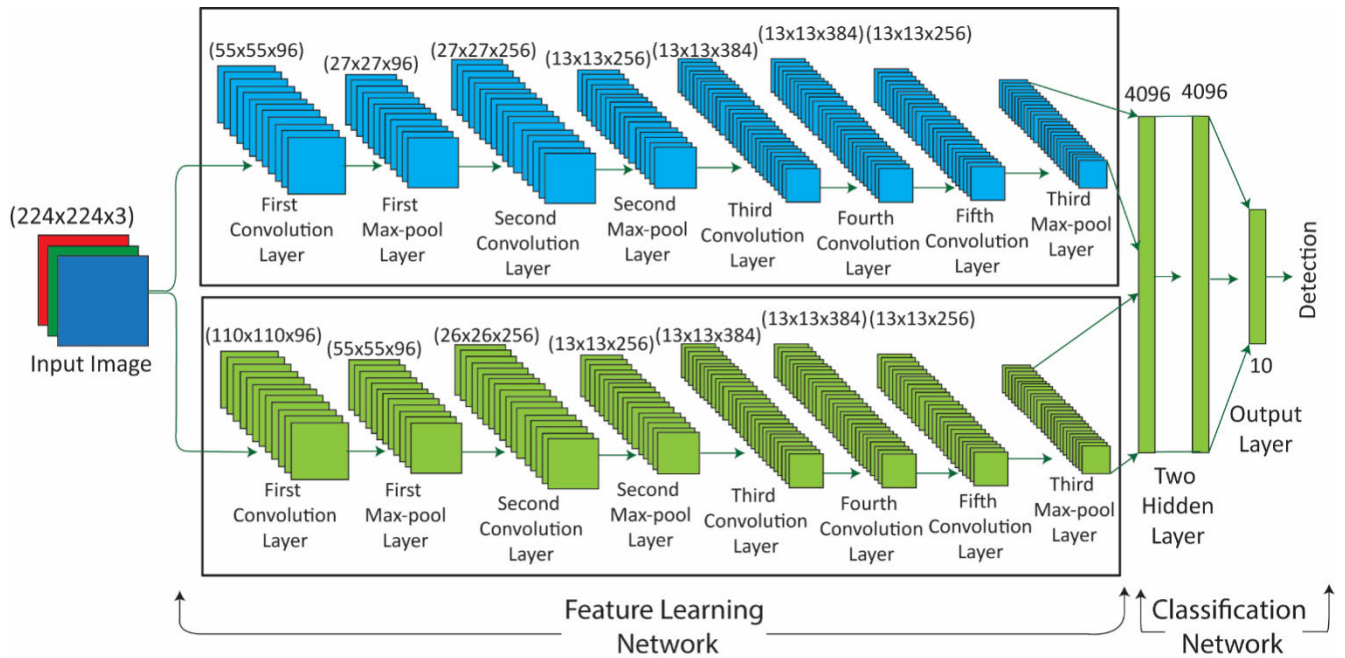


FIGURE 17. Proposed architecture of the convolution neural network.

TABLE 3. Summary of the CNN model.

Architecture	Layers	Feature Maps	Size	Kernel Size	Stride	Activation Function
-	Input Image	3	224x224	-	-	-
AlexNet	Convolution1	96	55x55	11x11	4x4	ReLU
ZFNet	Convolution6	96	110x110	7x7	2x2	ReLU
AlexNet	Max-pooling1	96	27x27	3x3	2x2	-
ZFNet	Max-pooling4	96	55x55	7x7	2x2	-
AlexNet	Convolution2	256	27x27	5x5	1x1	ReLU
ZFNet	Convolution7	256	26x26	3x3	2x2	ReLU
AlexNet	Max-pooling2	256	13x13	3x3	2x2	-
ZFNet	Max-pooling5	256	13x13	3x3	2x2	-
AlexNet	Convolution3	384	13x13	3x3	1x1	ReLU
ZFNet	Convolution8	384	13x13	3x3	1x1	ReLU
AlexNet	Convolution4	384	13x13	3x3	1x1	ReLU
ZFNet	Convolution9	384	13x13	3x3	1x1	ReLU
AlexNet	Convolution5	256	13x13	3x3	1x1	ReLU
ZFNet	Convolution10	256	13x13	3x3	1x1	ReLU
AlexNet	Max-pooling3	256	6x6	3x3	2x2	-
ZFNet	Max-pooling6	256	6x6	3x3	2x2	-
-	Concatenate	512	6x6	-	-	-
-	Flatten	1x1	18432	-	-	-
-	Hidden Layer1	1x1	4096	-	-	-
-	Hidden Layer2	1x1	4096	-	-	-
-	Output Layer	1x1	10	-	-	-

layers of ZFNet named with “Max-pooling4 to 6”. We concatenate the result after max-pooling layers 3, and 5 then processes for the further layers.

E. MOVEMENT IDENTIFICATION

For classification, we trained the CNN model with images of ten ankle exercise activities together. The ankle activity image with the high probability value identified as the correct output. So, we used a test dataset to test the trained model. All the used images identified by the trained CNN model correctly.

The accuracy rate of our proposed CNN model described in the results and discussion section.

V. METHODOLOGY

A. USRP HARDWARE SETUP

The hardware operation divided into two parts, and they are the transmitter side and the receiver side. Transmitter side consists of digital up-conversion (DUC), digital to analog conversion (DAC), low pass filtering (LPF), mixer, and transmit amplification (TA) to set the transmitter gain. On the

other side, the receiver side consists of low noise amplification (LNA), analog to digital converter (ADC), digital down converter (DDC), mixer, and log-periodic antenna (LPA). Lots of USRP devices available where we used the USRP B210 bus series, which was developed by Ettus Research and more about the device is available in [57]. We used two PC for the transmitter and receiver, where both have the same configuration, and they are Lenovo with Intel(R) Core (TM)i5-7500, 8 GB RAM, Windows 10 operating system. In our experiment, two USRP devices used and in experiment time, both attached with PC with the cable. In Table 4, we presented the hardware specification of used USRP.

TABLE 4. Hardware specification.

Name	B210
Antenna	Omni-direction
Frequency Range	70MHz-6GHz
Channel Mapping Rx	2
Channel Mapping Tx	2
Centre Frequency	5.32GHz
Master Clock Rate	200MHz
Interpolation Factor	250
Transport Data Type	int16
Decimation Factor	250
Transmitter Serial Number	30AD2AB
Receiver Serial Number	30AD3AL
Transmitter Gain	70
Receiver Gain	50
Samples Per Frames	80

**B. SOFTWARE SETUP**

In this research, we used MATLAB/Simulink version R2018a as a software to perform along with the USRP device for activity detection. The software part build of two main blocks, and they are the transmitter block and the receiver block. In Figure 18, we presented the transmitter and the receiver block of the software.

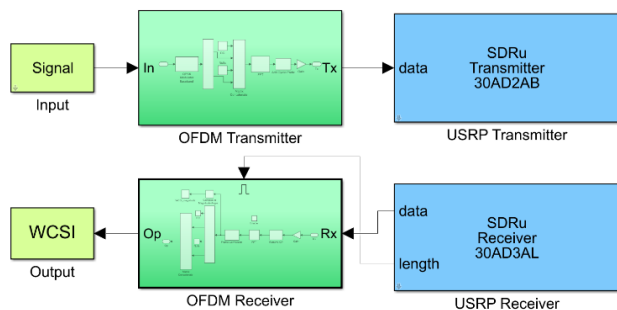


FIGURE 18. Block diagram of the Simulink model.

In prior research works [16], [17], several types of parameters used to build the software part. In our research, based

on the literature [27], we finalize the software parameters. Binary random bits used as input to the OFDM transmitter block, and it creates the OFDM symbols then apply the USRP transmitter block to send the signals. The transmitted signal received by the USRP receiver block then using the frequency response by utilizing the FFT at the receiver end to extract WCSI. In Table 5, we presented the software parameters used in the experiment.

TABLE 5. Software parameters.

Parameter	Values or Types
Input Bits	104
Modulation Type	QPSK
Bits Per Symbols (M)	2
Data Subcarrier	52
OFDM Subcarrier	64
Null Subcarrier	11
Used Subcarrier	52
DC	1
NFFT	64
Cyclic Prefix	NFFT-Data Subcarriers
Sampling Frequency	80e3
Samples Per Frames	80

**1) TRANSMITTER PROCEDURE**

In Figure 19, we presented a transmitter operation where bits created and information maps in a vector of bits. This vector of bits converted to a corresponding vector of integer values and modulated utilizing the quadrature phase-shift keying (QPSK) modulation technique. QPSK block accepts column or scalar vector input signal, and the input signal must be bits or integers.

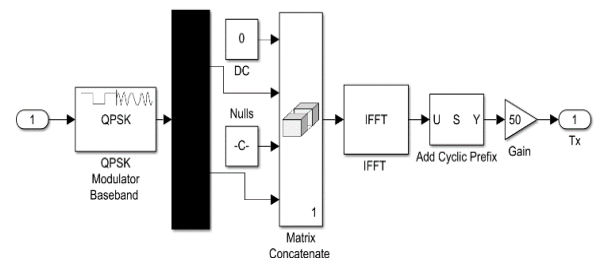


FIGURE 19. Block diagram of the transmitter process.

If the setting of the ‘Input Type’ is ‘Bit,’ then width needs to be an integer multiple of the total of bits of each symbol. De-mux block used to separate vector signals to a scalar or smaller vector and then used for convert series to parallel. After that to produce a continuous output signal, DC and Null subcarrier added. IFFT block added, which used to perform orthogonality between the subcarriers and to convert complex frequency domain signals to the time domain. In the end,

the cyclic prefix is added to prevent inter-symbol interference (ISI) and then forwarded it to the USRP hardware block for up-conversion and digital to analog conversion (DAC).

## 2) RECEIVER PROCEDURE

In Figure 20, we presented receiver operation where after down-sampling and analog to digital conversion (ADC), the first cyclic prefix removed from the USRP receiver block. Then FFT used to change the time domain into the frequency domain signal and phase and magnitude of the received signal calculated in the frequency domain. De-mux block used to separate vector signals to a scalar or smaller vector and then used for convert series to parallel. DC and Null subcarriers removed and demodulate the signal using QPSK then finally map a vector of bits. Above discussion, it can be said that the receiver procedure is the reverse of the transmitter procedure.

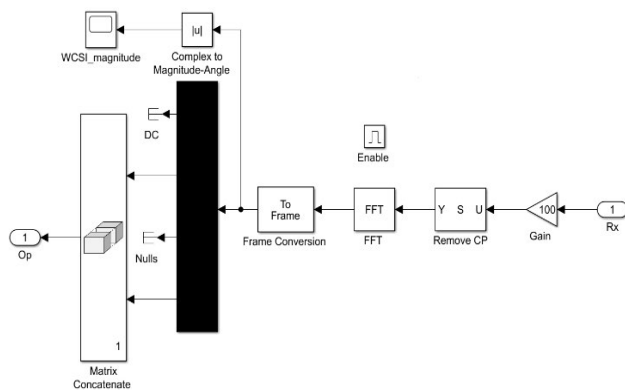


FIGURE 20. Block diagram of the receiver process.

## C. EXPERIMENTAL SETUP

For this research, we performed our experiments at Xidian University in the “Internet of Things” Lab, China. We used two desktop PC along with two USRP device. Both USRP devices equipped with one Omni-directional antenna. Selected subjects performed all activities of ankle exercises between the transmitting and receiving antenna. Subjects instructed to perform each ankle exercise five times, according to Table 2. Our used lab fully furnished where the table, sofa, and shelf were available. The length and the width of the experimental area are 7m and 5m, respectively, and the distance between transmitting antenna and receiving antenna is 120cm. Both USRP device placed on two separate small tables and the height of those tables are 50cm. One person always stays behind the pc to control software and collecting data. We allowed other students to enter the lab for work while experimenting. The typical scenario of the experimental setup presented in Figure 21.

## D. DATA ACCUMULATION

In the research, we used WCSI based ankle activities images to classify using the CNN model. To collect data on activities, we select ten human subjects with IRB approval. From the

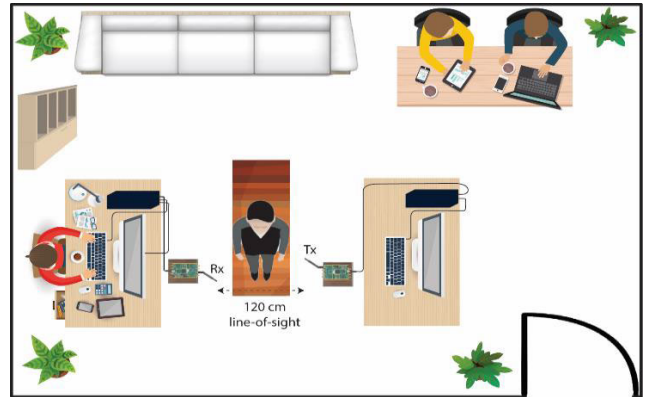


FIGURE 21. A typical scenario of the experiment setup.

ten subjects, six are males, and four are females, and their ages between 25 to 35. All the subjects instructed to perform activity five-time between the transmitter and the receiver in the proper way according to ankle exercises (refer to Table 2). Ten subjects performed ten activities of ankle exercises five times so, a total of 500 times activities performed. Our used WCSI technique has 64 subcarriers, and we plot each subcarrier and convert it into images, which means 64 subcarriers equal to 64 images. Now, if we multiply the 500 total number of times ten activity performed with 64 subcarriers, then we can get 32,000 subcarriers, which means 32,000 images used for classification. All the images divided into the train, validation, and test part then fed them into the CNN model. We used 60% images for the train, 20% images for the validation, and 20% images for the test so, randomly 19,200 images selected for the train, 6400 images for the validation, and 6400 images selected for the test.

## VI. RESULT AND DISCUSSION

### A. EXPERIMENTAL RESULT

In this section of this paper, we presented the result of the experiment of ten activities of ankle exercises after classification. We have ten activities, which means we have ten classes, and we used the short name of all the classes according to Table 2. We mainly focus on the classification result of our used CNN model. We provide the classification result of machine learning algorithms to describe the comparisons. To classify images, we used Python 3.7 version as a programming language; Anaconda to create and run the project; Keras, Tensorflow, and Scikit learn library to build CNN and CUDA enabled NVIDIA GPU to increase the performance.

### 1) RESULT OF CNN

With the help of layers of CNN, the classification rate goes high. We used AlexNet and ZFNet in a parallel manner to increase the accuracy rate high because both architectures have a certain number of layers. The input shape of the image is  $224 \times 224$  pixels, and the number of epochs is 20, where every epoch defines the number times that the learning algorithm worked with the full training dataset. We used

TABLE 6. Confusion matrix of test accuracy result.

Actual Class	Predicted Class									
	NWBD	NWBF	NWBI	NWBE	RSD	RSPF	RSI	RSE	PWBSCR	FWBSLS
NWBD	640	0	0	0	0	0	0	0	0	0
NWBF	0	640	0	0	0	0	0	0	0	0
NWBI	0	0	640	0	0	0	0	0	0	0
NWBE	0	0	0	640	0	0	0	0	0	0
RSD	0	0	0	0	632	0	0	0	8	0
RSPF	6	0	0	0	0	617	0	17	0	0
RSI	0	0	0	0	0	0	631	0	9	0
RSE	0	0	0	0	0	25	0	615	0	0
PWBSCR	0	0	0	0	0	0	0	0	640	0
FWBSLS	0	0	0	0	0	0	0	0	0	640

32000 images and split then into train, validation, and test (60% train, 20% validation, and 20% test) then classify using the CNN model. After classifying all the images of ten classes, we earned 98.98% test accuracy. In Table 6, we presented the confusion matrix of ten classes based on test accuracy result and in the confusion matrix, we used the short name of all ankle exercises according to Table 2.

From Table 6, we can see that 8 data of RSD mismatched with PWBSCR. Total 23 data of RSPF mismatched with two other activities where 6 mismatched with NWBD and 17 mismatched with RSE. 9 data of RSI mismatched with PWBSCR activity and 25 data of RSE mismatched with RSPF. There is no mismatched in the data of NWBD, NWBF, NWBI, NWBE, PWBSCR, and FWBSLS. In prior research (like [79], [80]), different kinds of methods used to measure the prediction performance. To evaluate classification results and the model properly, we exploit widely used metrics and they are sensitivity, specificity, Mathew’s correlation coefficient (MCC), precision (PR), recall (RE) and f1-score (F1). Sensitivity defined by  $Sensitivity = TP / (TP + FN) = TPR$ ; specificity defined by  $Specificity = TN / (TN + FP) = TNR$ ; Mathew’s correlation coefficient defined by  $MCC = ((TP * TN) - (FP * FN)) / \sqrt{((TP + FP) * (TP + FN) * (TN + FP) * (TN + FN))}$ ; precision defined by  $PR = TP / (TP + FP)$ ; the recall defined by  $RE = TP / (TP + FN)$  and f1-score defined by  $F1 = 2 * (PR * RE) / (PR + RE)$ . TP, TN, FP, and FN stand for true positive, true negative, false positive, and false negative respectively. In Table 7, we presented the sensitivity, specificity, Mathew’s correlation coefficient, precision, recall, and f1-score of the ten ankle exercises.

In Figure 22, we presented a ROC curve with the AUC score of ten classes. ROC curve and AUC score help to figure out the significant performance of a model. From Figure 22, we can say that our ROC curve of ten classes reached the ideal point. The AUC score stays between 0.96, 0.97, and 0.98. Class 2, 3, 8 and 9 has AUC score 0.98; class 0 and 1 has AUC score 0.97 an class 4, 5, 6 and 7 has AUC score 0.96. From the ROC curve and AUC score, it is showing that our CNN model achieved a significant level.

TABLE 7. Software sensitivity, specificity, MCC, precision, recall, and F1-score of ten classes.

Class	Sensitivity	Specificity	MCC	PR	RE	F1
NWBD	1	0.99	0.99	0.99	1	0.99
NWBF	1	1	1	1	1	1
NWBI	1	1	1	1	1	1
NWBE	1	1	1	1	1	1
RSD	0.98	1	0.99	1	0.98	0.99
RSPF	0.96	0.99	0.95	0.96	0.96	0.96
RSI	0.98	1	0.99	1	0.98	0.99
RSE	0.96	0.99	0.96	0.97	0.96	0.96
PWBSCR	1	0.99	0.98	0.97	1	0.98
FWBSLS	1	1	1	1	1	1

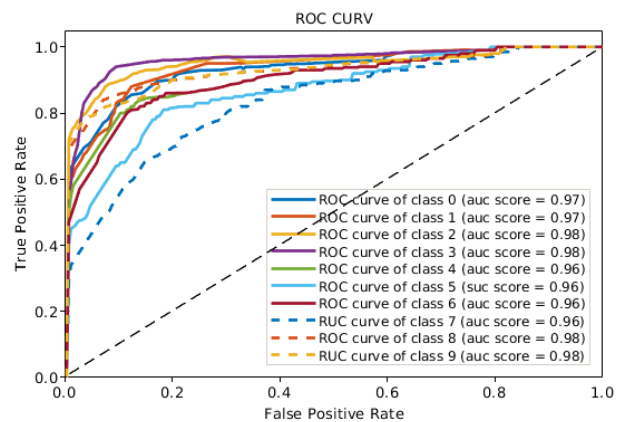


FIGURE 22. ROC curve for multi-classification of ten classes.

class 0 and 1 has AUC score 0.97 an class 4, 5, 6 and 7 has AUC score 0.96. From the ROC curve and AUC score, it is showing that our CNN model achieved a significant level.

2) RESULT OF ML

In prior research works [12], [13], different types of machine learning algorithms used for signal classification tasks [81]–[83]. We used four machine learning algorithms to

**TABLE 8. Accuracy result using machine-learning algorithms.**

Algorithms	Accuracy
SVM (with rbf)	92.67%
k-NN5	94.56%
DT	96.00%
PCA+SVM (with rbf)	88.00%
PCA+k-NN5	89.33%

classify WCSI data. They are support vector machine (SVM) with rbf kernel function, k-nearest neighbor (k-NN) with the value of  $k = 5$ , decision tree (DT), and principal component analysis (PCA). We run SVM and k-NN along with PCA. We presented the accuracy result using machine learning algorithms in Table 8.

From Table 8, we see that DT performs better than other algorithms, and the accuracy is 96%. In contrast, PCA with SVM and k-NN performed low where PCA with SVM has 88% accuracy, and PCA with k-NN has 89.33% accuracy. After DT, k-NN with the value of  $k = 5$  achieved 94.56% accuracy, and then SVM with rbf kernel function achieved 92.67% accuracy. To understand more about the performance of the used algorithms, we presented algorithm wise accuracy results and Mathew’s correlation coefficient (MCC) result of every single class in Table 9.

From Table 9, we can observe that the accuracy of class NWBD, NWBF, NWBI, NWBE, RSD, RSI, PWBSCR, and FWBSLS is very high in each algorithm. In contrast, the accuracy result of class RSPF and RSE is relatively lower than in other classes. Similarly, the correlation of class RSPF and RSE not high, like other classes. However, class NWBD, NWBF, NWBI, NWBE, RSD, RSI, PWBSCR, and FWBSLS have a higher and very strong positive correlation.

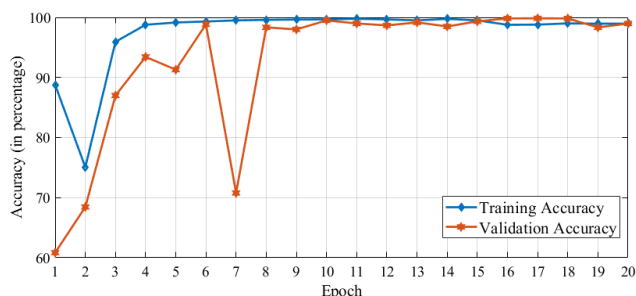
**B. DISCUSSION**

In this section, we discuss the classification accuracy results. We used two architecture in a parallel manner in the CNN

**TABLE 9. Algorithm wise accuracy result (Acc) and MCC result of 10 class.**

Class	SVM		k-NN5		DT		PCA+SVM		PCA+k-NN5	
	Acc	MCC	Acc	MCC	Acc	MCC	Acc	MCC	Acc	MCC
NWBD	0.98	0.93	0.98	0.93	0.99	0.95	0.98	0.90	0.98	0.91
NWBF	1	1	1	1	1	1	1	1	1	1
NWBI	1	1	1	1	1	1	0.99	0.95	0.99	0.97
NWBE	1	1	1	1	1	1	1	1	1	1
RSD	1	1	1	1	1	1	0.99	0.94	0.99	0.97
RSPF	0.93	0.65	0.94	0.69	0.96	0.80	0.90	0.55	0.91	0.56
RSI	0.98	0.93	0.99	0.95	0.99	0.97	0.97	0.88	0.98	0.90
RSE	0.95	0.70	0.95	0.75	0.97	0.85	0.92	0.47	0.92	0.54
PWBSCR	0.98	0.94	0.99	0.95	0.99	0.97	0.98	0.93	0.98	0.93
FWBSLS	1	1	1	1	1	1	1	1	1	1

model then used for classifying color images. We decided the number of epochs is 20. We split the 80% data to train and validate the model, where 60% used to train the model, and 20% used to validate the trained model. After that, we used the rest 20% images to test the trained model and get the test accuracy (98.98%), which used as an accuracy result. We get training accuracy and validation accuracy and training loss and validation loss after trained the model. In Figure 23, we presented the training accuracy and validation accuracy of every 20 epochs.



**FIGURE 23. Training accuracy and validation accuracy in 20 epochs.**

From Figure 23, we can observe that training accuracy in epoch 1 is 88.77% then it decreases at epoch 2. After epoch 2, from epoch 3 till the end, the training accuracy stays above 95%. At epoch 20, the training accuracy is 98.30%. On the other side, validation accuracy is 60.84% at epoch 1, and then it increases gradually until epoch 6. At epoch 7, validation accuracy dropped to 70.78%, and after that from epoch 8 to till the end validation accuracy stays above 97%. At epoch 20, the validation accuracy is 98.98%. In Figure 24, we presented the training loss and validation loss of every 20 epochs.

From Figure 24, we can observe that the training loss at epoch 1 is 0.29, and then it increases little at epoch 2.

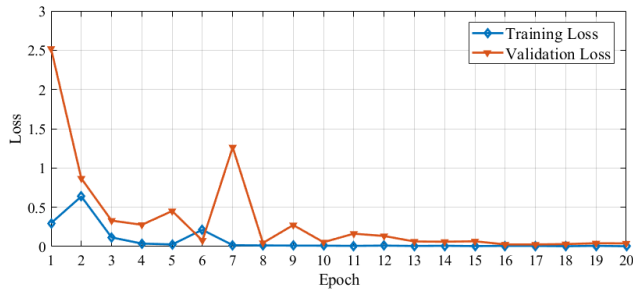


FIGURE 24. Training accuracy and validation loss in 20 epochs.

After that, it decreases slowly until the end with little fluctuation. In the end, the training loss of epoch 20 is 0.036. In contrast, validation loss at epoch 1 is 2.52, and then it gradually decreases until epoch 6. At epoch 7, the validation loss increased to 1.26, and after that, it decreases slowly until the end. At epoch 20, the validation loss is 0.04. Training loss and the validation loss helps to understand the overfitting problem of the model.

C. COMPARISON

We used CNN, which is built on two architecture to classify WCSI based image data and performed classification using ML algorithms to compare the accuracy result of CNN. After observing the classification result, we see that the accuracy result of CNN is better than ML algorithms. We gained a 98.98% accuracy result using CNN, where the accuracy result of ML algorithms stays below 96%. We classify the same dataset using AlexNet and ZFNet individually and compare the result. In Table 10, we presented the training accuracy, validation accuracy, test accuracy, training loss, and validation loss of AlexNet, ZFNet individually, and in a parallel manner of both architectures to make the comparison.

TABLE 10. List of training accuracy, test accuracy, training loss, and validation loss for comparison.

Features	AlexNet	ZFNet	AlexNet+ZFNet
Training Accuracy	96.61	97.39	98.30
Validation Accuracy	97.65	97.96	98.98
Test Accuracy	97.81	98.12	98.98
Training Loss	0.055	0.080	0.036
Validation Loss	0.093	0.031	0.040

From Table 10, we can observe that with the same dataset, AlexNet, and ZFNet performed well though in a parallel manner both architecture performed better than individually. The difference between training loss and validation loss of individual AlexNet and ZFNet is not satisfactory because it leads the model to overfitting or underfitting. In contrast, in a parallel manner of both architectures, the difference between training loss and validation loss is so low. We compare our accuracy result with prior research works where the SDR platform based USRP device and CNN model used to classify

images converted from signals (wireless signals, radio signals) data. In Table 11, we presented prior works to make the comparison.

TABLE 11. List of prior works for comparison.

Literature	Dataset (Based on)	Method	Accuracy
Soltani et al.[16]	Wireless Signal	CNN	94%
Schmidt et al.[17]	Wireless Signal	1D-CNN	98%
Wang et al.[25]	Wireless Signal	CNN+LSTM	95%
Liu et al.[21]	Wireless Signal	CLDNN	88.5%
Sedeghi et al.[84]	Radio Signal	VT-CNN2	93%
Kulin et al.[85]	Wireless Signal	CNN	98%

From Table 11, we can say that our proposed method gained better accuracy (98.98%) than given previous research works. In [16], they used embedded system (Deep Radio), which built with USRP N210 device to transmit and receive signals and used simple CNN model to classify and identify signals. In [17], they used USRP N210 device with LabVIEW and used 1D CNN model to classify and identify signals. In [25], they used USRP N210 device with LabVIEW and used CNN and LSTM model together for classification and identification. In [21], [84], [85], they implement GNU Radio using USRP device for transmit and receive signals, and to classify signals they develop simple CNN model. In contrast, instead of embedded system like [16], we used USRP B210 individually for transmitting and receiving. We implement software part in the Matlab software instead of using complex platform like LabVIEW and GNU Radio. In prior works like [16], [17], [85], simple CNN model where we build a complex CNN model where two architecture works in a parallel manner. We did not add any extra supporting model like [25], [21], [84] with our CNN model to enhance the accuracy.

VII. CONCLUSION

In this research paper, we proposed a healthcare system based on the convolutional neural network using two architectures in a parallel way to classify images and monitoring fractured ankle activity after surgery. We used WCSI based images to classify using CNN. WCSI based monitoring is a popular application for cognitive computing and communication. The principal novelty of this research work stays in the design of healthcare system to monitor fractured ankle movements after surgery, uses of USRP technology to capture WCSI data from wireless signals, and uses of two tested architectures in a parallel manner to build the CNN model. We used ten human subjects to perform the experiment, and then collated WCSI for classification using the CNN model. The classification result of our CNN model satisfies us, where the test accuracy is 98.98%, training accuracy is 98.30%, validation accuracy is 98.98% and we consider test accuracy as concluding result. This paper compares the accuracy results of the proposed CNN model and ML algorithms and compare with used models of prior works. Therefore, based on the

classification result, we can say that the use of CNN and USRP can make a good contribution to design healthcare monitoring systems. More use of USRP in healthcare application and design of the proper CNN model to detect the wrong exercise; to informing to do exercise at correct speed; to monitor how well patients are doing exercises considered as future work.

## REFERENCES

- [1] K. Hwang, M. Chen, H. Gharavi, and V. C. M. Leung, "Artificial intelligence for cognitive wireless communications," *IEEE Wireless Commun.*, vol. 26, no. 3, pp. 10–11, Jun. 2019.
- [2] M. Chen, F. Herrera, and K. Hwang, "Cognitive computing: Architecture, technologies and intelligent applications," *IEEE Access*, vol. 6, pp. 19774–19783, 2018.
- [3] E. Al Nuaimi, H. Al Neyadi, N. Mohamed, and J. Al-Jaroodi, "Applications of big data to smart cities," *J. Internet Services Appl.*, vol. 6, no. 1, p. 25, Dec. 2015.
- [4] L. Catarinucci, D. De Donno, L. Mainetti, L. Palano, L. Patrono, M. L. Stefanizzi, and L. Tarricone, "An IoT-Aware architecture for smart healthcare systems," *IEEE Internet Things J.* vol. 2, no. 6, pp. 515–526, Mar. 2015.
- [5] Y. Zhang, M. Chen, N. Guizani, D. Wu, and V. C. M. Leung, "SOVCAN: Safety-oriented vehicular controller area network," *IEEE Commun. Mag.*, vol. 55, no. 8, pp. 94–99, Aug. 2017.
- [6] Y. Zhang, M. Qiu, C.-W. Tsai, M. M. Hassan, and A. Alamri, "Health-CPS: Healthcare cyber-physical system assisted by cloud and big data," *IEEE Syst. J.*, vol. 11, no. 1, pp. 88–95, Mar. 2017.
- [7] M. Amiribesheli, A. Benmansour, and A. Bouchachia, "A review of smart homes in healthcare," *J. Ambient Intell. Humanized Comput.*, vol. 6, no. 4, pp. 495–517, Aug. 2015.
- [8] S. A. Shah, X. Yang, and Q. H. Abbasi, "Cognitive health care system and its application in pill-rolling assessment," *Int. J. Numer. Model., Electron. Netw., Devices Fields*, vol. 32, no. 6, e2632, Nov. 2019.
- [9] C. Souza, E. Pizzolato, R. Mendes, A. Borghi-Silva, M. Machado, and P. Correa, "Artificial neural networks prognostic evaluation of post-surgery complications in patients underwent to coronary artery bypass graft surgery," in *Proc. Int. Conf. Mach. Learn. Appl.*, Dec. 2009, pp. 799–803.
- [10] D. Haider, X. Yang, and Q. H. Abbasi, "Post-surgical fall detection by exploiting the 5 G C-band technology for eHealth paradigm," *Appl. Soft Comput.*, vol. 81, Aug. 2019, Art. no. 105537.
- [11] J. M. Medina McKeon and M. C. Hoch, "The ankle-joint complex: A kinesiologic approach to lateral ankle sprains," *J. Athletic Training*, vol. 54, no. 6, pp. 589–602, Jun. 2019.
- [12] J. Hayman, S. Prasad, and D. Stulberg, "Help patients prevent repeat ankle injury," *J. Family Pract.*, vol. 59, no. 1, p. 32, 2010.
- [13] W. Wang, A. X. Liu, and M. Shahzad, "Gait recognition using WiFi signals," in *Proc. ACM Int. Joint Conf. Pervas. Ubiquitous Comput.*, Sep. 2016, pp. 363–373.
- [14] A. Barua, X. Yang, A. Ren, D. Fan, L. Guan, N. Zhao, and D. Haider, "Gait signals classification and comparison," *Int. J. Numer. Model., Electron. Netw., Devices Fields*, vol. 32, no. 6, p. e2577, 2019.
- [15] X. Yang, S. A. Shah, A. Ren, N. Zhao, D. Fan, F. Hu, M. U. Rehman, K. M. von Deneen, and J. Tian, "Wandering pattern sensing at S-band," *IEEE J. Biomed. Health Informat.*, vol. 22, no. 6, pp. 1863–1870, Nov. 2018.
- [16] S. Soltani, Y. E. Sagduyu, R. Hasan, K. Davaslioglu, H. Deng, and T. Erpek, "Real-time and embedded deep learning on FPGA for RF signal classification," 2019, *arXiv:1910.05765*. [Online]. Available: <http://arxiv.org/abs/1910.05765>
- [17] E. Schmidt, D. Inupakutika, R. Mundlamuri, and D. Akopian, "SDR-Fi: Deep-learning-based indoor positioning via software-defined radio," *IEEE Access*, vol. 7, pp. 145784–145797, 2019.
- [18] Z. Liu, L. Wang, W. Liu, and B. Li, "Human movement detection and gait periodicity analysis using channel state information," in *Proc. 12th Int. Conf. Mobile Ad-Hoc Sensor Netw. (MSN)*, Dec. 2016, pp. 167–174.
- [19] Y. Bengio, "Learning deep architectures for AI," *Found. Trends Mach. Learn.*, vol. 2, no. 1, pp. 1–127, 2009.
- [20] L. Deng, "A tutorial survey of architectures, algorithms, and applications for deep learning," *APSIPA Trans. Signal Inf. Process.*, vol. 3, nos. 3–4, pp. 1–29, Jun. 2014.
- [21] X. Liu, D. Yang, and A. E. Gamal, "Deep neural network architectures for modulation classification," in *Proc. 51st Asilomar Conf. Signals, Syst., Comput.*, Oct. 2017, pp. 915–919.
- [22] Y. LeCun, Y. Bengio, and G. Hinton, "Deep learning," *Nature*, vol. 521, no. 7553, pp. 436–444, 2015.
- [23] M. Y. W. Teow, "Understanding convolutional neural networks using a minimal model for handwritten digit recognition," in *Proc. IEEE 2nd Int. Conf. Autom. Control Intell. Syst. (I CACIS)*, Oct. 2017, pp. 167–172.
- [24] S. Dörner, S. Cammerer, J. Hoydis, and S. T. Brink, "Deep learning based communication over the air," *IEEE J. Sel. Topics Signal Process.*, vol. 12, no. 1, pp. 132–143, Feb. 2018.
- [25] Q. Wang, P. Du, T. Dou, L. Gao, and C. Li, "Cognitive passive radar system: Software defined radio and deep learning approach," *J. Eng.*, vol. 2019, no. 21, pp. 7326–7330, Nov. 2019.
- [26] F. Paisana, A. Selim, M. Kist, P. Alvarez, J. Tallon, C. Bluemm, A. Puschmann, and L. DaSilva, "Context-aware cognitive radio using deep learning," in *Proc. IEEE Int. Symp. Dyn. Spectr. Access Netw. (DySPAN)*, Mar. 2017, pp. 1–2.
- [27] M. B. Khan, X. Yang, A. Ren, M. A. M. Al-Hababi, N. Zhao, L. Guan, D. Fan, and S. A. Shah, "Design of software defined radios based platform for activity recognition," *IEEE Access*, vol. 7, pp. 31083–31088, 2019.
- [28] D. Wang, A. Khosla, R. Gargeya, H. Irshad, and A. H. Beck, "Deep learning for identifying metastatic breast cancer," 2016, *arXiv:1606.05718*. [Online]. Available: <http://arxiv.org/abs/1606.05718>
- [29] D. George and E. A. Huerta, "Deep neural networks to enable real-time multimessenger astrophysics," *Phys. Rev. D, Part. Fields*, vol. 97, no. 4, Feb. 2018, Art. no. 044039.
- [30] D. Silver, A. Huang, C. J. Maddison, A. Guez, L. Sifre, G. van den Driessche, J. Schrittwieser, I. Antonoglou, V. Panneershelvam, M. Lanctot, S. Dieleman, D. Grewe, J. Nham, N. Kalchbrenner, I. Sutskever, T. Lillicrap, M. Leach, K. Kavukcuoglu, T. Graepel, and D. Hassabis, "Mastering the game of go with deep neural networks and tree search," *Nature*, vol. 529, no. 7587, p. 484, 2016.
- [31] M. Borgerding and P. Schniter, "Onsager-corrected deep learning for sparse linear inverse problems," in *Proc. IEEE Global Conf. Signal Inf. Process. (GlobalSIP)*, Dec. 2016, pp. 227–231.
- [32] Y.-S. Jeon, S.-N. Hong, and N. Lee, "Blind detection for MIMO systems with low-resolution ADCs using supervised learning," in *Proc. IEEE Int. Conf. Commun. (ICC)*, May 2017, pp. 1–6.
- [33] N. Farsad and A. Goldsmith, "Detection algorithms for communication systems using deep learning," 2017, *arXiv:1705.08044*. [Online]. Available: <http://arxiv.org/abs/1705.08044>
- [34] J. Wang, Y. Ma, L. Zhang, R. X. Gao, and D. Wu, "Deep learning for smart manufacturing: Methods and applications," *J. Manuf. Syst.*, vol. 48, pp. 144–156, Jul. 2018.
- [35] U. M. Khan, Z. Kabir, S. A. Hassan, and S. H. Ahmed, "A deep learning framework using passive WiFi sensing for respiration monitoring," in *Proc. IEEE Global Commun. Conf. (GLOBECOM)*, Dec. 2017, pp. 1–6.
- [36] D. Haider, A. Ren, D. Fan, N. Zhao, X. Yang, S. A. K. Tanoli, Z. Zhang, F. Hu, S. A. Shah, and Q. H. Abbasi, "Utilizing a 5G spectrum for health care to detect the tremors and breathing activity for multiple sclerosis," *Trans. Emerg. Telecommun. Technol.*, vol. 29, no. 10, p. e3454, Oct. 2018.
- [37] R. Gao, J. Xue, W. Xiao, B. Zhao, and S. Zhang, "Extreme learning machine ensemble for CSI based device-free indoor localization," in *Proc. 28th Wireless Opt. Commun. Conf. (WOCC)*, May 2019, pp. 1–5.
- [38] M. M. H. Ali, V. H. Mahale, P. Yannawar, and A. T. Gaikwad, "Overview of fingerprint recognition system," in *Proc. Int. Conf. Electr., Electron., Optim. Techn. (ICEEOT)*, Mar. 2016, pp. 1334–1338.
- [39] P. Kumari, L. Mathew, and P. Syal, "Increasing trend of wearables and multimodal interface for human activity monitoring: A review," *Biosensors Bioelectron.*, vol. 90, pp. 298–307, Apr. 2017.
- [40] S. Zhang, Z. Wei, J. Nie, L. Huang, S. Wang, and Z. Li, "A review on human activity recognition using vision-based method," *J. Healthcare Eng.*, vol. 2017, pp. 1–31, Jul. 2017.

- [41] C. Wang, J. Zhang, L. Wang, J. Pu, and X. Yuan, "Human identification using temporal information preserving gait template," *IEEE Trans. Pattern Anal. Mach. Intell.*, vol. 34, no. 11, pp. 2164–2176, Nov. 2012.
- [42] L. Wang, T. Tan, H. Ning, and W. Hu, "Silhouette analysis-based gait recognition for human identification," *IEEE Trans. Pattern Anal. Mach. Intell.*, vol. 25, no. 12, pp. 1505–1518, Dec. 2003.
- [43] J. Mantyjarvi, J. Himberg, and T. Seppanen, "Recognizing human motion with multiple acceleration sensors," in *Proc. IEEE Int. Conf. Syst., Man Cybern. E-Syst. E-Man Cybern. Cyberspace*, vol. 2, Oct. 2001, pp. 747–752.
- [44] R. Vera-Rodriguez, J. S. D. Mason, J. Fierrez, and J. Ortega-Garcia, "Comparative analysis and fusion of spatiotemporal information for footstep recognition," *IEEE Trans. Pattern Anal. Mach. Intell.*, vol. 35, no. 4, pp. 823–834, Apr. 2013.
- [45] M. Otero, "Application of a continuous wave radar for human gait recognition," in *Proc. 16th Signal Process., Sensor Fusion, Target Recognit.*, vol. 5809, May 2005, pp. 538–548.
- [46] F. Adib, C.-Y. Hsu, H. Mao, D. Katabi, and F. Durand, "Capturing the human figure through a wall," *ACM Trans. Graph.*, vol. 34, no. 6, pp. 1–13, Nov. 2015.
- [47] B. Kellogg, V. Talla, and S. Gollakota, "Bringing gesture recognition to all devices," in *Proc. 11th USENIX Symp. Netw. Syst. Design Implement. (NSDI)*, 2014, pp. 303–316.
- [48] K. Higuchi, H. Itaka, R. Sakamoto, and K. Yano, "Analysis of involuntary movement and development of a writing assistance system for adults with tension athetosis type cerebral palsy," in *Proc. IEEE Conf. Control Appl. (CCA)*, Oct. 2014, pp. 1294–1299.
- [49] X. Yang, D. Fan, A. Ren, N. Zhao, S. A. Shah, A. Alomainy, M. Ur-Rehman, and Q. H. Abbasi, "Diagnosis of the Hypopnea syndrome in the early stage," *Neural Comput. Appl.*, vol. 32, no. 3, pp. 1–12, 2019.
- [50] Y. Wang, K. Wu, and L. M. Ni, "WiFall: Device-free fall detection by wireless networks," *IEEE Trans. Mobile Comput.*, vol. 16, no. 2, pp. 581–594, Feb. 2017.
- [51] Y. Wang, J. Liu, Y. Chen, M. Gruteser, J. Yang, and H. Liu, "E-eyes: Device-free location-oriented activity identification using fine-grained WiFi signatures," in *Proc. 20th Annu. Int. Conf. Mobile Comput. Netw. (MobiCom)*, 2014, pp. 617–628.
- [52] S. Shah, C. M. Blanchette, J. Noone, and E. A. Wikstrom, "Prevalence and burden of Ankle injuries in North Carolina emergency departments," *Value Health*, vol. 18, no. 3, p. A250, May 2015.
- [53] R. Bahr and I. A. Bahr, "Incidence of acute volleyball injuries: A prospective cohort study of injury mechanisms and risk factors," *Scandin. J. Med. Sci. Sports*, vol. 7, no. 3, pp. 166–171, Jan. 2007.
- [54] C. Milgrom, N. Shlankovitch, A. Finestone, A. Eldad, A. Laor, Y. L. Danon, O. Lavie, J. Wosk, and A. Simkin, "Risk factors for lateral ankle sprain: A prospective study among military recruits," *Foot Ankle*, vol. 12, no. 1, pp. 26–30, Aug. 1991.
- [55] N. Wedderkopp, M. Kaltoft, R. Holm, and K. Froberg, "Comparison of two intervention programmes in young female players in European handball—with and without ankle disc," *Scandin. J. Med. Sci. Sports*, vol. 13, no. 6, pp. 371–375, Dec. 2003.
- [56] W. H. Meeuwisse, H. Tyreman, B. Hagel, and C. Emery, "A dynamic model of etiology in sport injury: The recursive nature of risk and causation," *Clin. J. Sport Med.*, vol. 17, no. 3, pp. 215–219, May 2007.
- [57] D. Haider, A. Ren, D. Fan, N. Zhao, X. Yang, S. A. Shah, F. Hu, and Q. H. Abbasi, "An efficient monitoring of eclamptic seizures in wireless sensors networks," *Comput. Electr. Eng.*, vol. 75, pp. 16–30, May 2019.
- [58] M. W. O. Brien, J. S. Harris, O. Popescu, and D. C. Popescu, "An experimental study of the transmit power for a USRP software-defined radio," in *Proc. Int. Conf. Commun. (COMM)*, Jun. 2018, pp. 377–380.
- [59] F. Al-Turjman, "Intelligence and security in big 5G-oriented IoNT: An overview," *Future Gener. Comput. Syst.*, vol. 102, pp. 357–368, Jan. 2020.
- [60] D. F. Fioranelli, D. S. A. Shah, H. Li, A. Shrestha, D. S. Yang, and D. J. Le Kernec, "Radar sensing for healthcare," *Electron. Lett.*, vol. 55, no. 19, pp. 1022–1024, Sep. 2019.
- [61] F. Fioranelli, J. Le Kernec, and S. A. Shah, "Radar for health care: Recognizing human activities and monitoring vital signs," *IEEE Potentials*, vol. 38, no. 4, pp. 16–23, Jul. 2019.
- [62] S. Aziz Shah, J. Ahmad, A. Tahir, F. Ahmed, G. Russell, S. Y. Shah, W. J. Buchanan, and Q. H. Abbasi, "Privacy-preserving non-wearable occupancy monitoring system exploiting Wi-Fi imaging for next-generation body centric communication," *Micromachines*, vol. 11, no. 4, p. 379, Apr. 2020.
- [63] S. A. K. Tanoli, M. I. Khan, Q. Fraz, X. Yang, and S. A. Shah, "A compact beam-scanning leaky-wave antenna with improved performance," *IEEE Antennas Wireless Propag. Lett.*, vol. 17, no. 5, pp. 825–828, May 2018.
- [64] S. A. Shah and F. Fioranelli, "RF sensing technologies for assisted daily living in healthcare: A comprehensive review," *IEEE Aerosp. Electron. Syst. Mag.*, vol. 34, no. 11, pp. 26–44, Nov. 2019.
- [65] F. Al-Turjman, M. H. Nawaz, and U. D. Ulusar, "Intelligence in the Internet of medical things era: A systematic review of current and future trends," *Comput. Commun.*, vol. 150, pp. 644–660, Jan. 2020.
- [66] A. Tahir, J. Ahmad, S. A. Shah, G. Morison, D. A. Skelton, H. Larjani, Q. H. Abbasi, M. A. Imran, and R. M. Gibson, "WiFreeze: Multiresolution scalograms for freezing of gait detection in Parkinson's leveraging 5G spectrum with deep learning," *Electronics*, vol. 8, no. 12, p. 1433, Dec. 2019.
- [67] T. B. Welch and S. Shearman, "Teaching software defined radio using the USRP and LabVIEW," in *Proc. IEEE Int. Conf. Acoust., Speech Signal Process. (ICASSP)*, Mar. 2012, pp. 2789–2792.
- [68] J. Yang, M. N. Nguyen, P. P. San, X. L. Li, and S. Krishnaswamy, "Deep convolutional neural networks on multichannel time series for human activity recognition," in *Proc. 24th Int. Joint Conf. Artif. Intell.*, Jun. 2015, pp. 3995–4001.
- [69] T. Zebin, P. J. Scully, and K. B. Ozanyan, "Human activity recognition with inertial sensors using a deep learning approach," in *Proc. IEEE SENSORS*, Oct. 2016, pp. 1–3.
- [70] S. Jacob, V. G. Menon, F. Al-Turjman, P. G. Vinoj, and L. Mostarda, "Artificial muscle intelligence system with deep learning for post-stroke assistance and rehabilitation," *IEEE Access*, vol. 7, pp. 133463–133473, 2019.
- [71] F. Ordóñez and D. Roggen, "Deep convolutional and LSTM recurrent neural networks for multimodal wearable activity recognition," *Sensors*, vol. 16, no. 1, p. 115, Jan. 2016.
- [72] N.-Q.-K. Le, Q.-T. Ho, and Y.-Y. Ou, "Incorporating deep learning with convolutional neural networks and position specific scoring matrices for identifying electron transport proteins," *J. Comput. Chem.*, vol. 38, no. 23, pp. 2000–2006, Sep. 2017.
- [73] N. Q. K. Le, T.-T. Huynh, E. K. Y. Yapp, and H.-Y. Yeh, "Identification of clathrin proteins by incorporating hyperparameter optimization in deep learning and PSSM profiles," *Comput. Methods Programs Biomed.*, vol. 177, pp. 81–88, Aug. 2019.
- [74] M. I. Jordan and T. M. Mitchell, "Machine learning: Trends, perspectives, and prospects," *Science*, vol. 349, no. 6245, pp. 255–260, Jul. 2015.
- [75] Y. LeCun, K. Kavukcuoglu, and C. Farabet, "Convolutional networks and applications in vision," in *Proc. IEEE Int. Symp. Circuits Syst.*, Jun. 2010, pp. 253–256.
- [76] L. Liu, S. Shah, G. Zhao, and X. Yang, "Respiration symptoms monitoring in body area networks," *Appl. Sci.*, vol. 8, no. 4, p. 568, Apr. 2018.
- [77] K. Simonyan and A. Zisserman, "Very deep convolutional networks for large-scale image recognition," 2014, *arXiv:1409.1556*. [Online]. Available: <http://arxiv.org/abs/1409.1556>
- [78] A. Krizhevsky, I. Sutskever, and G. E. Hinton, "ImageNet classification with deep convolutional neural networks," in *Proc. Adv. Neural Inf. Process. Syst. (NIPS)*, 2012, pp. 1097–1105.
- [79] A. Berg, J. Deng, and L. Fei-Fei, "Large scale visual recognition challenge (ILSVRC)," Springer Link, Cham, Switzerland, Tech. Rep. 115, 2010.
- [80] J. Deng, W. Dong, R. Socher, L.-J. Li, K. Li, and L. Fei-Fei, "ImageNet: A large-scale hierarchical image database," in *Proc. IEEE Conf. Comput. Vis. Pattern Recognit.*, Jun. 2009, pp. 248–255.
- [81] D. Haider, O. Romain, J. L. Kernec, S. Y. Shah, M. M. U. Farooq, and Z. Qadus, "Monitoring body motions related to huntington disease by exploiting the 5G paradigm," in *Proc. UK/China Emerg. Technol. (UCET)*, Aug. 2019, pp. 1–4.
- [82] S. A. Shah, D. Fan, A. Ren, N. Zhao, X. Yang, and S. A. K. Tanoli, "Seizure episodes detection via smart medical sensing system," *J. Ambient Intell. Humanized Comput.*, vol. 9, pp. 1–13, Nov. 2018.



[83] Q. Zhang, D. Haider, W. Wang, S. Shah, X. Yang, and Q. Abbasi, "Chronic obstructive pulmonary disease warning in the approximate ward environment," *Appl. Sci.*, vol. 8, no. 10, p. 1915, Oct. 2018.

[84] M. Sadeghi and E. G. Larsson, "Adversarial attacks on deep-learning based radio signal classification," *IEEE Wireless Commun. Lett.*, vol. 8, no. 1, pp. 213–216, Feb. 2019.

[85] M. Kulin, T. Kazaz, I. Moerman, and E. De Poorter, "End-to-end learning from spectrum data: A deep learning approach for wireless signal identification in spectrum monitoring applications," *IEEE Access*, vol. 6, pp. 18484–18501, 2018.



**FADI AL-TURJMAN** (Member, IEEE) received the Ph.D. degree in computer science from Queen's University, Kingston, ON, Canada, in 2011. He is a Full Professor and a Research Center Director of Near East University, Nicosia, Cyprus. He is a leading authority in the areas of smart/intelligent, wireless, and mobile networks' architectures, protocols, deployments, and performance evaluation. His publication history spans over 250 publications in journals, conferences, books, and book chapters, in addition to numerous keynote and plenary talks at flagship venues. He has authored and edited more than 25 books about cognition, security, and wireless sensor networks' deployments in smart environments, published by Taylor and Francis, Elsevier, and Springer. He has led a number of international symposia and workshops in flagship communication society's conferences. He has received several recognitions and best papers' awards at top international conferences. He also received the prestigious Best Research Paper Award for *Computer Communications* journal (Elsevier), from 2015 to 2018, in addition to the Top Researcher Award from Antalya Bilim University, Turkey, in 2018. He serves as an Associate Editor and the Lead Guest/Associate Editor for several well-reputed journals, including the *IEEE COMMUNICATIONS SURVEYS AND TUTORIALS* (IF 22.9) and *Sustainable Cities and Society* (IF 4.7) (Elsevier).



**ARNAB BARUA** is currently with Xidian University.



**ZHI-YA ZHANG** was born in Jiangsu, China, in 1985. He received the B.S. degree in electrical engineering and the Ph.D. degree in electromagnetic field and microwave technology from Xidian University, Xi'an, China, in 2007 and 2012, respectively. He works as an Associate Professor with the National Key Laboratory of Antennas and Microwave Technology, Xidian University. His current research interests include broadband antennas, millimeter-wave antennas, and antenna arrays.



**XIAODONG YANG** (Senior Member, IEEE) has published over 100 articles in peer-reviewed journals. He has a global collaborative research network in his research related fields. His main research interests include body area networks. He received the Young Scientist Award from the International Union of Radio Science, in 2014. He serves on the editorial board of several IEEE and IET journals.

...